

University of Groningen

Bypass of a protein barrier by a replicative DNA helicase

Yardimci, Hasan; Wang, Xindan; Loveland, Anna B.; Tappin, Inger; Rudner, David Z.; Hurwitz, Jerard; van Oijen, Antoine M.; Walter, Johannes C.

Published in:
Nature

DOI:
[10.1038/nature11730](https://doi.org/10.1038/nature11730)

IMPORTANT NOTE: You are advised to consult the publisher's version (publisher's PDF) if you wish to cite from it. Please check the document version below.

Document Version
Publisher's PDF, also known as Version of record

Publication date:
2012

[Link to publication in University of Groningen/UMCG research database](#)

Citation for published version (APA):

Yardimci, H., Wang, X., Loveland, A. B., Tappin, I., Rudner, D. Z., Hurwitz, J., van Oijen, A. M., & Walter, J. C. (2012). Bypass of a protein barrier by a replicative DNA helicase. *Nature*, 492(7428), 205-+. <https://doi.org/10.1038/nature11730>

Copyright

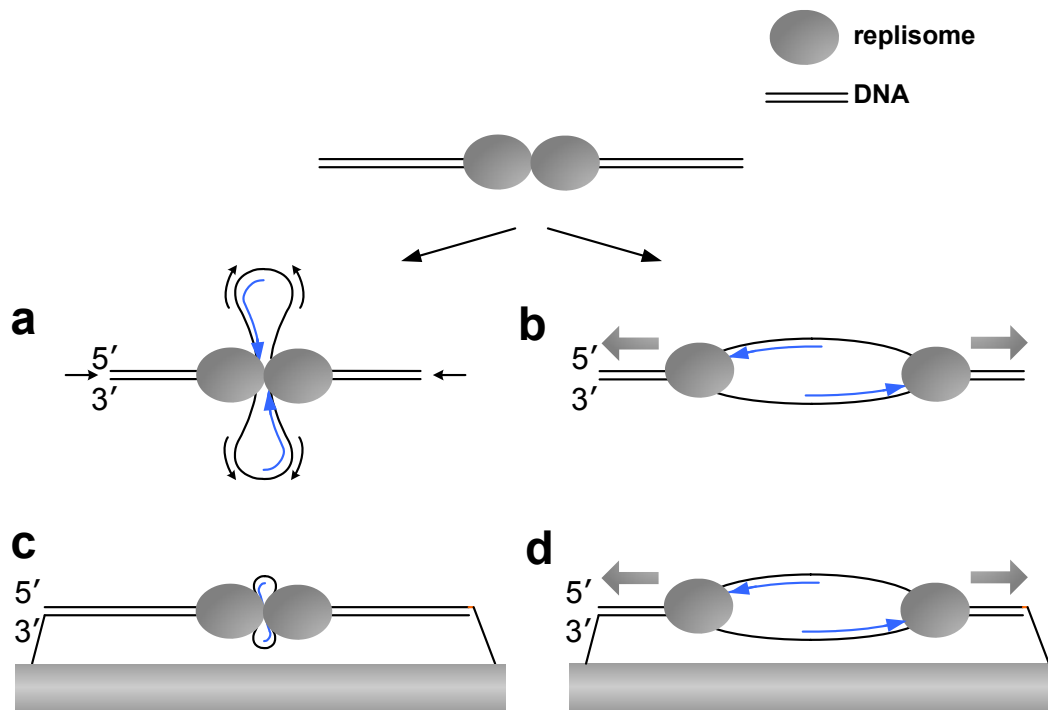
Other than for strictly personal use, it is not permitted to download or to forward/distribute the text or part of it without the consent of the author(s) and/or copyright holder(s), unless the work is under an open content license (like Creative Commons).

The publication may also be distributed here under the terms of Article 25fa of the Dutch Copyright Act, indicated by the "Taverne" license. More information can be found on the University of Groningen website: <https://www.rug.nl/library/open-access/self-archiving-pure/taverne-amendment>.

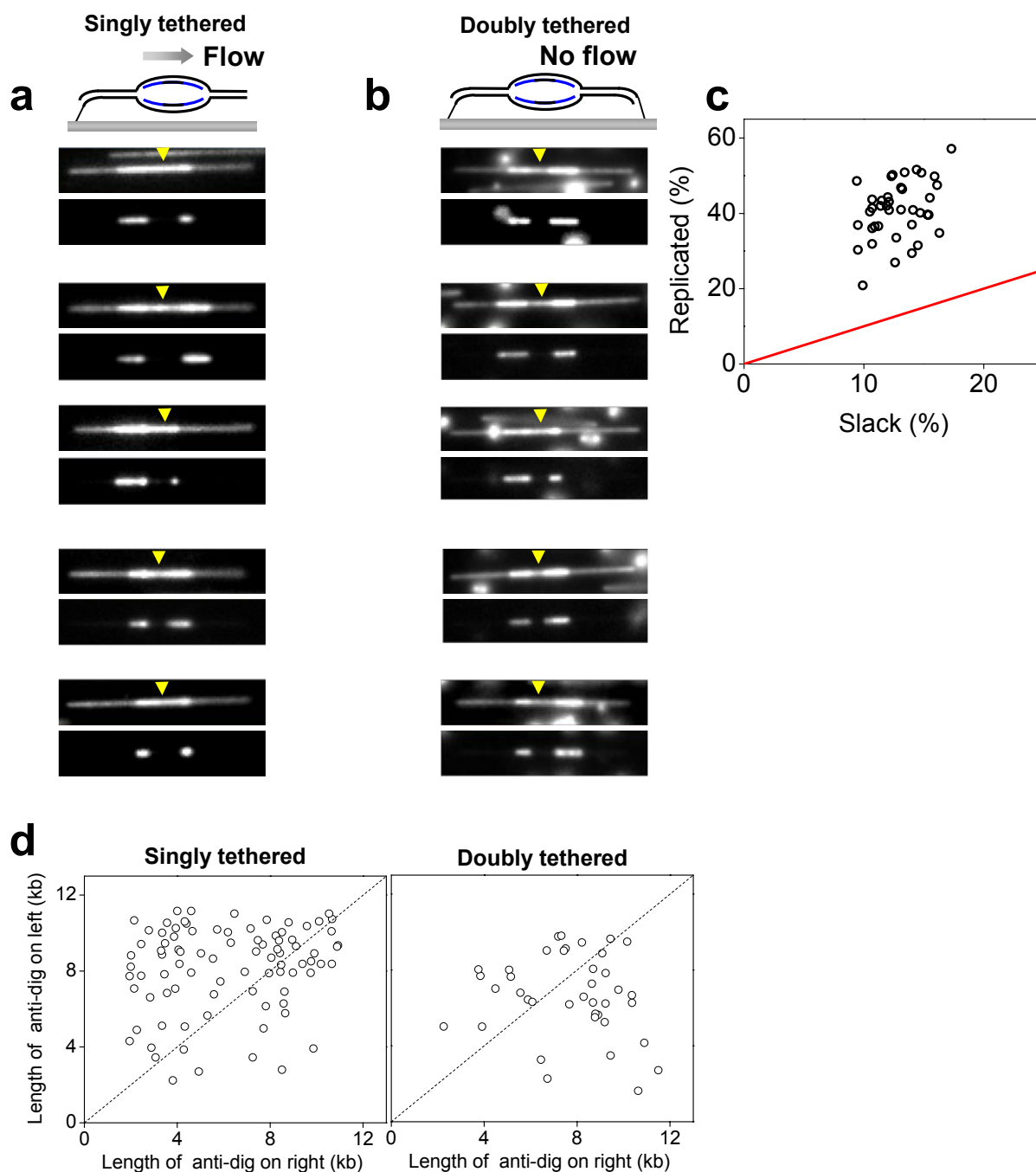
Take-down policy

If you believe that this document breaches copyright please contact us providing details, and we will remove access to the work immediately and investigate your claim.

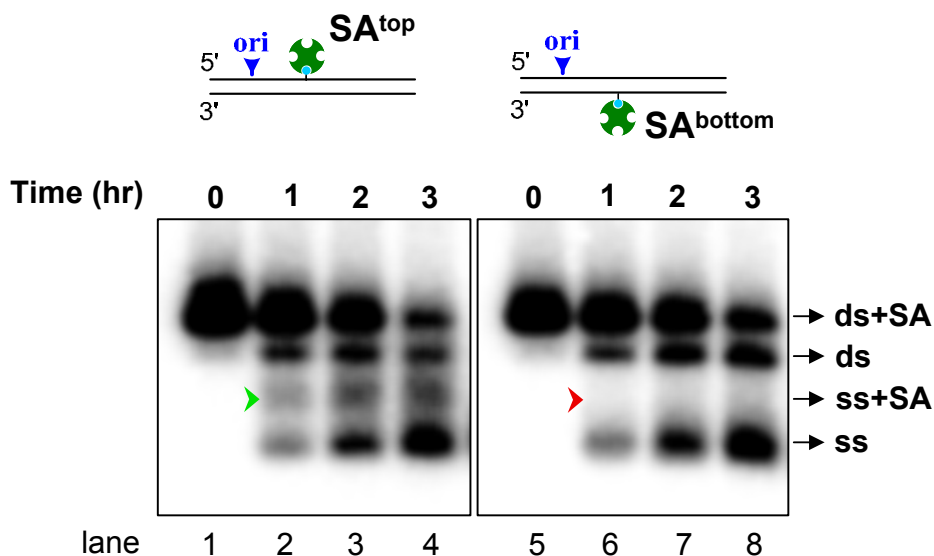
Downloaded from the University of Groningen/UMCG research database (Pure): <http://www.rug.nl/research/portal>. For technical reasons the number of authors shown on this cover page is limited to 10 maximum.



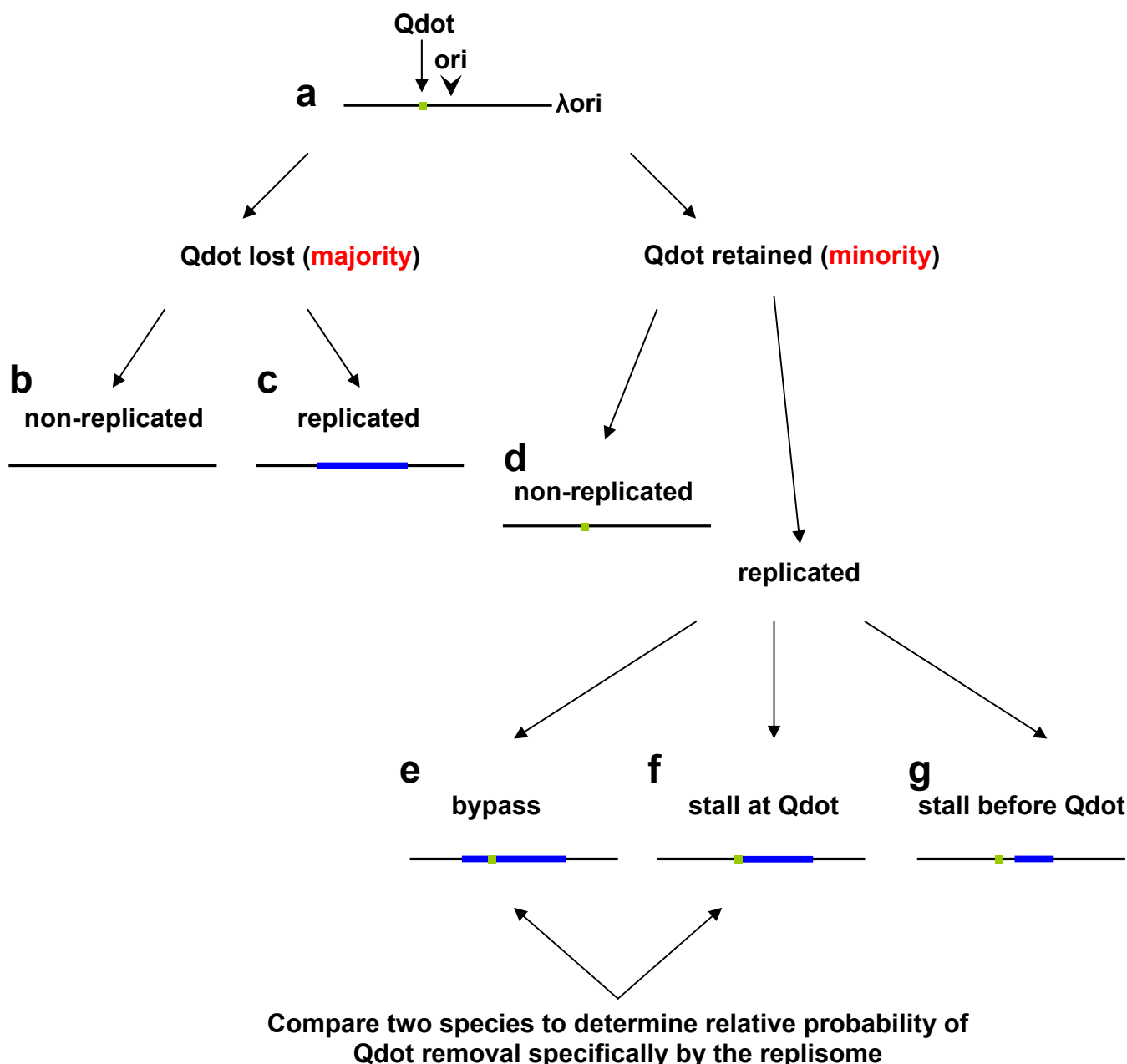
Supplementary Figure 1. **a-b**, Models depicting physically coupled (**a**) and autonomously functioning (**b**) sister replisomes. **c-d**, The double-replisome model predicts inefficient replication of stretched DNA (**c**), while independent replisomes should be able to replicate stretched DNA (**d**). Black arrows in **a** illustrate the movement of DNA and gray arrows in **b** and **d** show the direction of movement of replisomes. Blue lines depict leading strand synthesis.



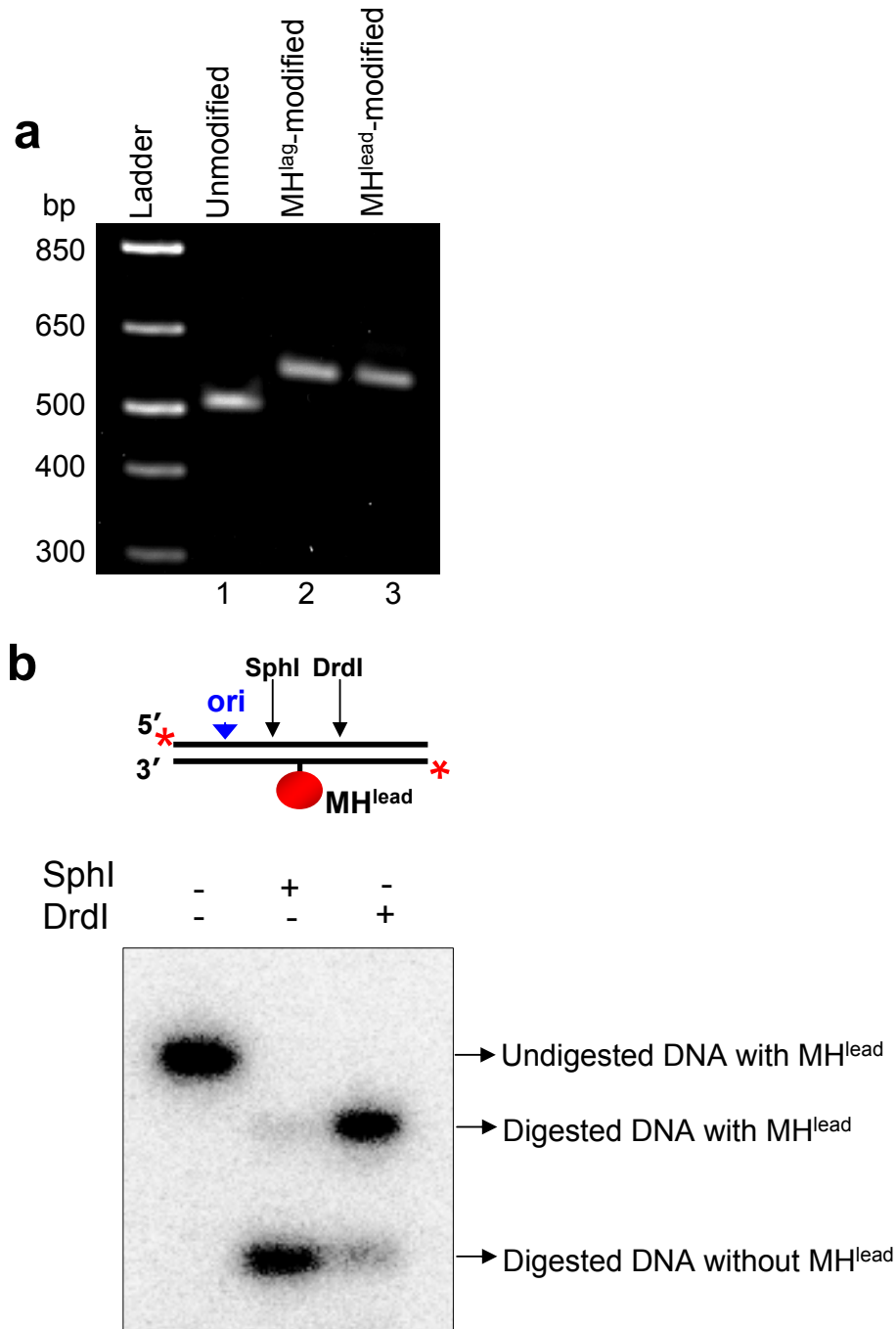
Supplementary Figure 2. T-ag-dependent replication of singly and doubly tethered λ ori DNA in HeLa cell extracts. **a-b**, Additional examples of singly (**a**) and doubly (**b**) tethered DNA molecules after replication, as in Fig. 1b. Yellow arrowheads indicate the predicted location of the SV40 origin. **c**, Extent of replication *versus* the initial slack present on doubly tethered DNA. The red line indicates the level of replication expected if replication were limited to the initial slack present in the molecule. **d**, Lengths of left *versus* right anti-dig tracts on singly and doubly tethered DNA. Dashed lines represent perfect correlation.



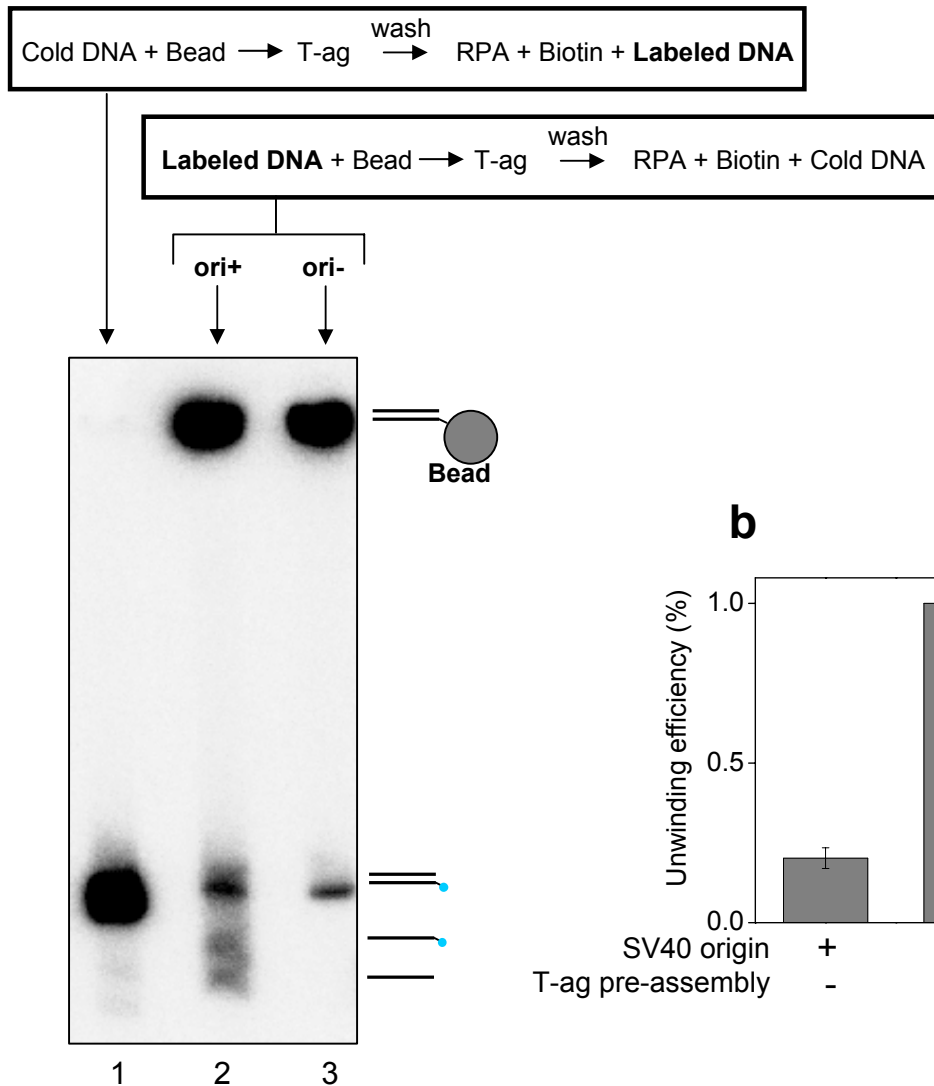
Supplementary Figure 3. Displacement of SA by T-ag. Internally radiolabeled DNA templates containing a biotin on the top (left panel) or bottom (right panel) strands were mixed with SA. T-ag and RPA were added to initiate unwinding. Excess biotin was also included to sequester free SA. Reactions were incubated for indicated periods of time at 37°C and subsequently kept at 4°C until all time points were collected. Reactions were terminated with 0.5% SDS and 20 mM EDTA, DNA was separated on a 3% agarose gel, and visualized using a phosphorimager. SA was more effectively displaced by T-ag from the bottom strand (lanes 6-8, red arrowhead) than it was from the top strand (lanes 2-4, green arrowhead) indicating that T-ag translocates on the leading strand template in the 3' to 5' direction.



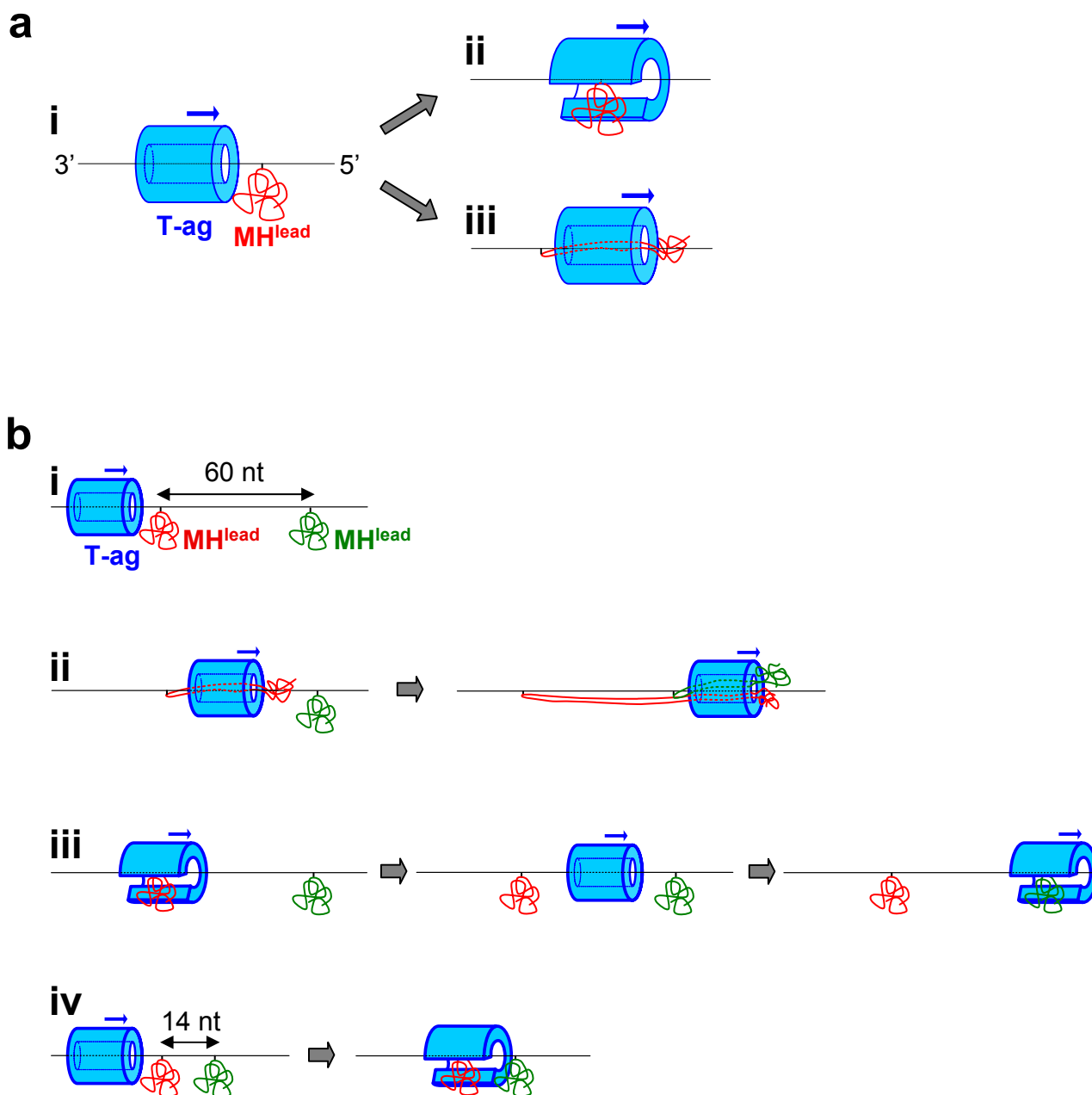
Supplementary Figure 4. Schematic illustration of DNA templates observed in replisome collisions with Qdots. Before the replication reaction, the DNA contains a Qdot (a). During the reaction, Qdots on the majority of DNA molecules were lost (b and c). Most Qdot dissociation events were independent of replication because extensive Qdot loss was also observed in the absence of extracts. A subset of molecules that retained the Qdot (d-g) contained a replication bubble (e-g). Within this group, we compared the fraction of molecules in which the anti-dig tract bypassed the Qdot (v; “bypass” in Fig. 2d) to those in which the end of the anti-dig tract co-localized with the Qdot (vi; “stall” in Fig. 2d). Because the probability of scoring species depicted in (vi) is the same for Qdot^{lead} and Qdot^{lag}, these molecules can serve as a reference to determine the probability of Qdot removal by the replisome. A fork was considered to be stalled at the Qdot if the end of the anti-dig tract was located within 2 pixels ($\sim 0.3 \mu\text{m}$) of the Qdot.



Supplementary Figure 5. a, DNA was modified with M.HpaII on the lagging (MH^{lag}) or leading (MH^{lead}) strand templates and purified as described in Supplementary Methods. Unmodified (lane 1), MH^{lag}-conjugated (lane 2), and MH^{lead}-conjugated (lane 3) templates were separated on a native agarose gel, stained with SYBR Gold (Invitrogen), and visualized with UV light. The complete mobility shift indicates that all DNA was modified with M.HpaII. **b**, 5'-radiolabeled DNA containing MH^{lead} was digested with SphI or DrrI, which cut on either side of the M.HpaII. DNA was separated on a native agarose gel and visualized by autoradiography. Results indicate that the top strand is more efficiently labeled than the bottom strand.

a**b**

Supplementary Figure 6. DNA unwinding by pre-assembled T-ag. **a**, Unlabeled ('cold') origin-containing DNA (lane 1), labeled origin-containing DNA (lane 2), or labeled originless DNA (lane 3) was immobilized on beads, T-ag was assembled, and free T-ag was then removed. Finally, RPA and labeled origin-containing DNA (lane 1) or cold origin-containing DNA (lanes 2 and 3) was added. The bands corresponding to each template are indicated. **b**, Quantification of unwinding from three independent experiments as in **a**. Error bars indicate standard deviation. The fact that the labeled origin DNA added after removal of free T-ag was inefficiently unwound (lane 1) indicates that DNA unwinding in lane 2 was largely carried out by pre-assembled T-ag. Furthermore, the absence of unwinding in lane 3 indicates that unwinding in lane 2 was origin-dependent.



Supplementary Figure 7. a, Models for roadblock bypass by T-ag. (i) T-ag (blue) collides with a M.Hpall roadblock (red) on the leading strand template. The blue arrow indicates the direction of T-ag movement. The excluded strand is not shown for simplicity. (ii) The T-ag ring opens to bypass the roadblock. (iii) T-ag denatures M.Hpall during translocation and threads the unfolded polypeptide chains of M.Hpall through its central channel. **b**, To differentiate between the T-ag opening and M.Hpall denaturation models, unwinding assays were performed on templates containing two MH^{lead} adducts separated by 60 nt (i). (ii) In the M.Hpall denaturation model, the central channel of T-ag would have to enclose four polypeptide chains and ssDNA to unwind a DNA containing two adducts. This conclusion is based on the following rationale:

because M.HpII (358 residues long) is linked to the DNA through residue 103, two polypeptides will enter T-ag's central channel when the helicase passes over the protein. To reach the end of the shorter of the two polypeptides, 102 amino acids ($\sim 370 \text{ \AA}$) would need to pass through the central channel. Since the roadblocks were placed only 60 nt apart, T-ag would encounter the second MH^{lead} molecule before it completely bypassed the short arm of the first MH^{lead} molecule, resulting in four polypeptide chains in the central channel. This argument holds true even if the translocation strand between the first and second adducts were extended to the contour length of B form DNA ($\sim 200 \text{ \AA}$), as depicted in the cartoon. (iii) The longitudinal axis of T-ag is 120 \AA long. Therefore, if the T-ag ring opens to undergo bypass, it can re-close before encountering the second roadblock located 60 nt away. (iv) When two adducts are spaced 14 nt ($\sim 50 \text{ \AA}$) apart, the hexamer collides with the second roadblock before it can re-close.